BIOMECHANICS

The role of sagittal alignment in predicting major failure of lumbopelvic instrumentation: a biomechanical validation of lumbopelvic failure classification

Woojin Cho[1] · Wenhai Wang[2] · Brandon Bucklen[2]

Abstract

Study design Finite element analysis.

Objectives To biomechanically validate the classification of lumbopelvic fixation failure using an in silico model.

Summary of background data Even though major failure of lumbopelvic constructs has occurred more often in patients with suboptimal lumbar lordosis and sagittal balance, there has been no biomechanical validation of this classification.

Methods Finite element models (T10–pelvis) were created to match the average spinal–pelvic parameters of two cohorts of patients reported in Cho et al. (J Neurosurg Spine 19:445–453, 2013): major failure group (defined as rod breakage between L4 and S1, failure of S1 screws and prominence of iliac screws requiring removal) and non-failure group. A moment was applied at the T10 superior endplate to simulate gravimetric loading in a standing position.

Results Due to differences in the alignment of spinopelvic parameters between normal and failed spines in the presence of a fixed gravity line, the major failure cohort in this study observed a 20% higher load and 18% greater instability. As a result, the rod and screw stress in the major failure cohort increased by 20% and 42%, respectively, in comparison to the non-failure cohort.

Conclusions The greater mechanical demand on the posterior rods in the lower lumbar spine in the major failure cohort further emphasizes the importance of proper sagittal alignment. This finite element analysis validates the classification of lumbopelvic fixation failure.

Keywords Lumbopelvic fixation · Finite element analysis · Lumbopelvic failure · Biomechanics · Sagittal alignment

Introduction

Surgical correction of adult spinal deformity (ASD) often requires a multilevel fusion ranging from the proximal level of L2 or higher to the pelvis. If fusion is not successful,

✉ Wenhai Wang
wwang@globusmedical.com

Woojin Cho
wcho@montefiore.org

Brandon Bucklen
bbucklen@globusmedical.com

[1] Albert Einstein College of Medicine/Montefiore Medical Center, 3400 Bainbridge Ave, 6th Fl., Bronx, NY 10461, USA

[2] Musculoskeletal Education and Research Center (MERC), A Division of Globus Medical, Inc., 2560 General Armistead Avenue, Audubon, PA 19403, USA

substantial biomechanical loading, particularly at the proximal or distal ends, can result in rod fracture (RF), screw pullout, or other failure. Literature reports that RF occurs in 6.8–9.3% of ASD patients, and for those who underwent pedicle subtraction osteotomy (PSO), the total incidence of RF was as high as 22% [1, 2]. In the case of lumbopelvic fixation after long construct fusion for ASD, Cho et al. [3] reported a 34.3% incidence of overall failure, with 11.9% of patients experiencing clinically significant major failure requiring a revision. As there was no consensus on the definition of lumbopelvic failure in the primary author's previous work, failure was defined as either major or minor failure [3]. Major failure included rod breakage between L4 and S1, failure of S1 screws (breakage, halo formation, or pullout), or prominent iliac screws which required revision surgery. Minor failure included rod breakage between S1 and iliac screws, or failure of iliac screws excluding prominence of iliac screws and did not require revision surgery.

Rod failure may be attributed to many factors such as: (1) rod material and diameter [2, 4]; (2) rod contouring techniques and achieved curvature [2, 4]; (3) patient pre-operative sagittal alignment, such as pelvic tilt (PT), sacral slope (SS), pelvic incidence (PI), and sagittal vertical axis (SVA) [2, 3, 5]; and (4) surgical technique-related factors such as choice of osteotomy or choice of distal foundation [2–4]. Although there is no agreement among researchers on which factor had the most impact on rod fractures, it is well known that sagittal alignment is a key factor in reducing abnormal loading on the spine, lessening the risk of RF. Sagittal alignment is usually assessed by a plumb line method drawn on full-length radiographs. Other methods, such as T1 and T9 spinopelvic inclination [5] or cranial sagittal vertical axis [6, 7] also have been used. Many studies have investigated the association between sagittal alignment and clinical outcomes [8–10]. There is overall agreement among those retrospective studies that positive sagittal alignment (SVA > 0) is associated with pain and disability. Emami et al. [11] demonstrated that patients with poor sagittal balance after long fusions to the sacrum had increased pain. Glassman et al. [8] reported that patients with positive sagittal imbalance expressed worse self-assessment in the SRS-22 questionnaire's pain, function, and self-image subscores. In the past, force-plate analysis has been used to capture the spinal and pelvic offsets from the standing foot position and to help evaluate sagittal imbalance [12]. The axis of the femoral shaft and the plumb line has also been evaluated for the imbalance prior to surgical correction [13].

Even though major failure of lumbopelvic constructs occurred more often in patients with suboptimal lumbar lordosis and sagittal balance, there has been no biomechanical validation of this classification. Questions remain regarding mechanical risk factors, or if there is any relationship between implant type, spinopelvic parameters, and failure

to achieve fusion. The purpose of this study is to biomechanically validate the classification of lumbopelvic fixation failure using an in silico model.

Materials and methods

The development of the finite element models involves three steps. In the first step, an L4–L5 FSU (functional spinal unit) finite element model was first developed and validated. The spine geometry was modified from a CAD model (Digimation, Inc., Lake Mary, FL, USA). Intervertebral disc was simplified as flat endplate. The cancellous core, posterior elements of the vertebrae, the annulus fibrosus, and the nucleus were modeled as three-dimensional isotropic four node tetrahedral solid elements (C3D4). Thin shell elements (S3R) with thicknesses of 0.5 mm and 0.3 mm were used to model the cortical shell and endplate, respectively. Material properties were obtained from several references and are listed in Table 1. The annulus fibrosus was modeled by a hyperelastic constitutive law for the ground substance and by nonlinear springs oriented at ± 30° to the horizontal for the annulus fibers [14]. Coefficients of the third-order Ogden hyperelastic formulation were determined from experimental data and used [15]. Facet cartilage was modeled as shell elements with a thickness of 0.3 mm [16]. Sliding interaction between facets was modeled as a frictionless contact. Six spinal ligaments were represented by three-dimensional unidirectional spring elements. A stepwise calibration was performed in the same sequence as reported by Schmidt et al. [17]. Material properties of each added component were modified to match the corresponding in vitro data point.

In the second step, the validated L4–L5 FSU finite element model was then extended to T12–pelvis by adding more vertebrae and the pelvis. The sacroiliac joint was

Table 1 Element type and material properties of the vertebrae used in the finite element model of the motion segment

Component name	Element type	Material properties	References
Cortical bone	4-Node solid	$E = 12{,}000$ MPa, $\upsilon = 0.3$	[14, 16]
Cancellous bone	4-Node solid	$E = 100$ MPa, $\upsilon = 0.2$	[14, 16]
Bony posterior elements	4-Node solid	$E = 3500$ MPa, $\upsilon = 0.25$	[14, 16]
Nucleus pulposus	4-Node solid	$E = 1$, $\upsilon = 0.499$	[14, 16]
Annulus	4-Node solid	Hyperelastic, Ogden 3rd material model	[14–16]
Ligaments	2-Node spring	ALL: $k = 2.5$ $n = 13$ PLL: $k = 0.1$ $n = 5$ FCL, FCR: $k = 1.5$ $n = 18$ FL: $k = 1.5$ $n = 7$ ISL: $k = 0.1$ $n = 5$ SSL: $k = 0.5$ $n = 3$	[14, 16]
Pedicle screws and rods	4-Node solid	$E = 113.8$ GPa, $\upsilon = 0.342$	

E, Young's modulus; υ, Poisson's ratio; k, spring constant; n, number of springs; ALL, anterior longitudinal ligament; PLL, posterior longitudinal ligament; FL, flaval ligament; SSL, supraspinous ligament; ISL, interspinous ligament; FC, facet capsular ligaments

modeled as articular cartilage contacts surrounded by six types of strong ligaments (anterior sacroiliac, interosseous sacroiliac, long posterior sacroiliac, short posterior sacroiliac, sacrospinous, sacrotuberous) [18], depicted as spring elements. The range of motion of the intact T12–pelvis spine unit was then validated against an in-house cadaveric test of six specimens. A maximum moment of ± 10 Nm was applied in flexion/extension, lateral bending, and axial rotation. The motion captured was comparable to the experimental measurements (Fig. 1).

In the last step, final T10–pelvis model was created to match the average spinal-pelvic parameters (PT, SS, and lumbar lordosis) of two cohorts of patients reported in the literature [3], major failure and non-failure groups (Fig. 2). The non-failure cohort had a mean post-operative SVA of 49.6 mm, placing it into the sagittal-forward alignment group (0–50 mm), and a mean gravity line (GL) offset from the heels of 110 mm [12]. The major failure group had a post-operative SVA of 70.3 mm, placing it into the sagittal-forward alignment group (> 50 mm), and a similar GL offset as the non-failure group. As shown in Fig. 2, the distance from the center of the hip joint to the center of the superior endplate of T10 was 57.7 mm and 59.0 mm in the non-failure and major failure groups in the sagittal plane, respectively. For the sagittal-forward group to maintain balance of the spinopelvic axis, pelvic retroversion (posterior shifting of the pelvis toward the heels to maintain a balanced mass distribution) has to occur [5]. In our model, we assumed that the pelvis was shifted toward the heel by 10 mm for the major failure group, which is quite conservative compared to the 30 mm pelvic shift for the sagittal-forward group observed in

the literature [5]. If we assume the average human weight is 75 kg and the upper body weight above T10 is about 40% of the whole body weight (~ 300 N), then the moment created by the upper body on the spine is this weight multiplied by the distance (D) between the GL and the center of the T10 superior endplate (moment = 300 N × D). Since the pelvis was shifted toward the heel by 10 mm in the major failure group, the moment arm was 69.0 mm compared to 57.7 mm in the non-failure group (Fig. 1). As the result, the non-failure group underwent 17.3 Nm moment loading while the major failure group underwent 20.7 Nm moment loading. The corresponding moment was applied to the superior endplate of T10 to simulate the static gravimetric loading in a standing position. No cyclic loading was simulated.

Results

Despite a fixed GL position relative to the heels, differences in spinopelvic parameters resulted in a neutral sagittal alignment in the non-failure spine model, but produced a sagittal-forward alignment in the major failure model. As a result, the bending moment was approximately 17.3 Nm in the non-failure group and 20.7 Nm in the major failure group, representing a 20% increase. Differences in loads produced 14 mm of translation and 4.9° of rotation for the major failure group—18% and 14% higher, respectively, compared to the non-failure group (11.9 mm translation and 4.3° rotation) (Fig. 3). For comparison purposes, the non-failure model was loaded with the same amount of moment applied to the major failure model (20.7 Nm) to isolate the effect of loading and alignment independently. The achieved translation and rotation were 13.2 mm and 4.7°, respectively—6% and 4% lower than the major failure group, respectively.

Rod stresses were highest at L1–L2 and L4–L5 in both cases. In the major failure group, maximum stress (138.3 MPa) was observed between L4 and L5. In the non-failure group, maximum stress (115.4 MPa) was at the surface between L1 and L2 (Fig. 4). High stress (141.0 MPa) was also observed in S1 screws in the major failure group. This value was 42% greater than the stress (98.9 MPa) observed in the non-failure group.

As with stress, high strain was also observed at L1–L2 and L4–L5 in both models (Fig. 5). The maximum strain was detected on the right rod surface between L4 and L5 in the major failure group and on the left rod surface between L4 and L5 in the non-failure group (0.13% and 0.11%, respectively). The average maximum rod surface strain was about 22% higher in the major failure group in comparison to the non-failure group. Additionally, noticeably high strain in the S1 screw was observed. Results were 0.13% for the major failure group—42% higher than the S1 screw strain (0.09%) observed in the non-failure group.
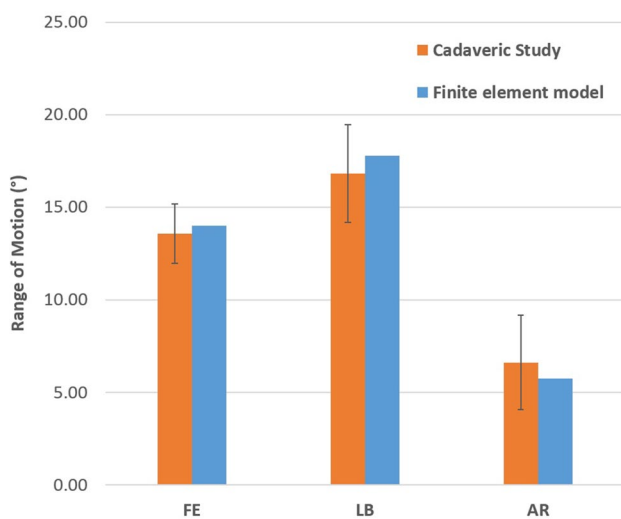

Fig. 1 Comparison of range of motion of the intact spine unit between the in vitro biomechanical test and simulation result of finite element model under 10 Nm moment in flexion/extension (FE), lateral bending (LB), and axial rotation (AR)
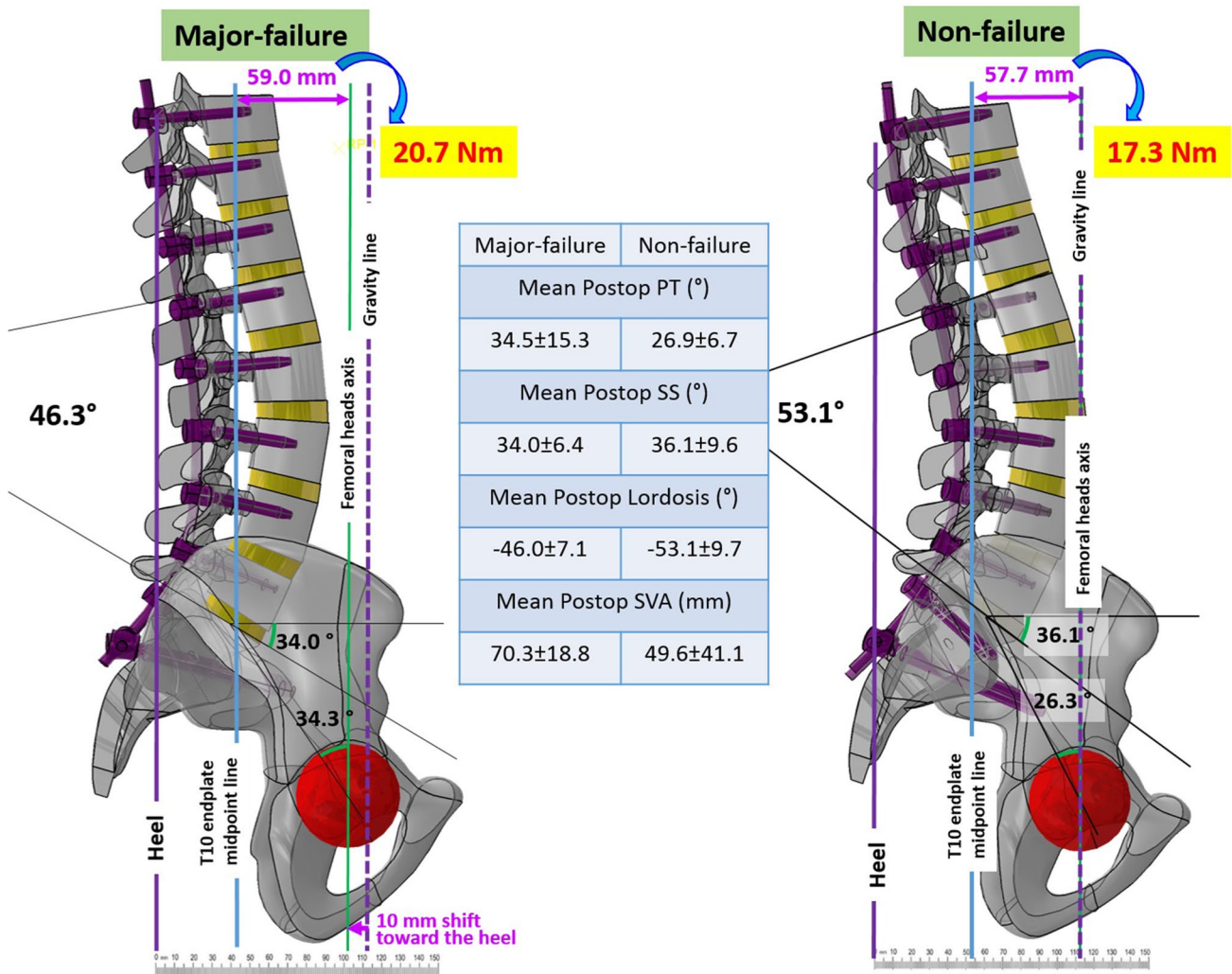
Fig. 2 Finite element models for major failure and non-failure cohorts; values listed in the table are extracted from the retrospective study conducted by Cho et al. [3]. PT = the angle between the vertical and the line through the midpoint of the sacral plate to femoral heads axis; SS = the angle between the horizontal and the sacral plate; SVA = the offset from C7 plumb line and the posterosuperior corner of S1

Discussion

In the current study, an in silico model was used to validate the major failure and non-failure classifications of lumbopelvic fixation described by Cho et al. [3]. Patients with major failure risk factors—including larger PI, decreased lumbar lordosis (LL), and much higher SVA—demonstrated a greater likelihood for sagittal imbalance when compared to the non-failure group. From a biomechanical point of view, the major failure group observed a 20% increase in loading due to the fixed gravity line, which led to a 14% and 18% increase in rotation and translation, as well as a 20% increase in rod stress/strain when compared to the non-failure group. For the major failure group to maintain balance, pelvic retroversion/shift had to occur [5]. Pelvic shift (in relation to the feet) is an important component in maintaining a somewhat

fixed GL-heels offset, even in the setting of variable SVA and trunk inclination [12]. This mechanism uses muscle force to improve alignment, and thereby restore the GL position and horizontal gaze [19]. In this case, the pelvis shift was modeled at 10 mm. However, clinically, sagittal-forward patients with pelvic shifts greater than 30 mm have been observed [5], which would have increased the gravimetric load by up to 54%. In this worst-case scenario, dramatic increases in rotation, translation, and stress concentration on the rod and screw would be expected. Generally speaking, the more pelvic retroversion, the greater the shift of the pelvis toward the heel, resulting in a greater moment arm between the GL and the lumbopelvic spine, increased muscle activity, and greater load on the construct.

Assessing SVA alone may underestimate the severity of the deformity [20]. Schwab et al. [20] reported that the
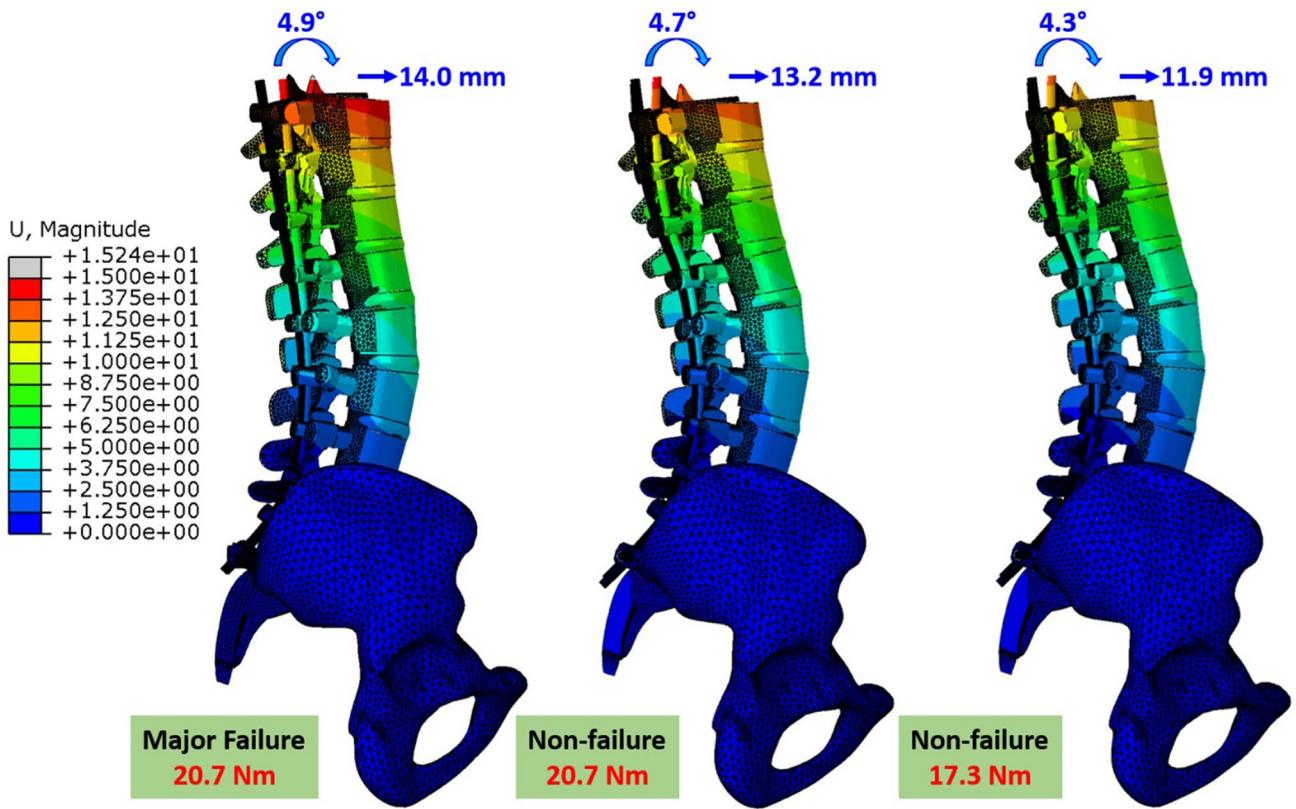
Fig. 3 Load and displacement comparison between major failure and non-failure groups

Fig. 4 Rod and screw stress contours under the gravitational loading; values shown in the figure are average surface von Mises stresses. Units are MPa
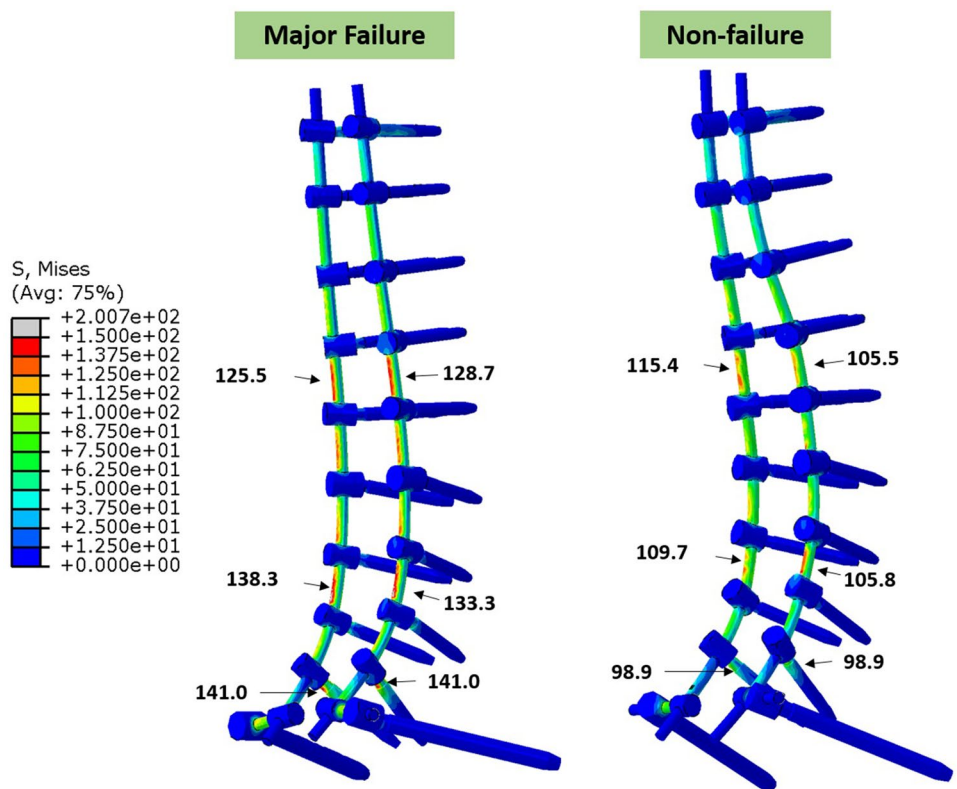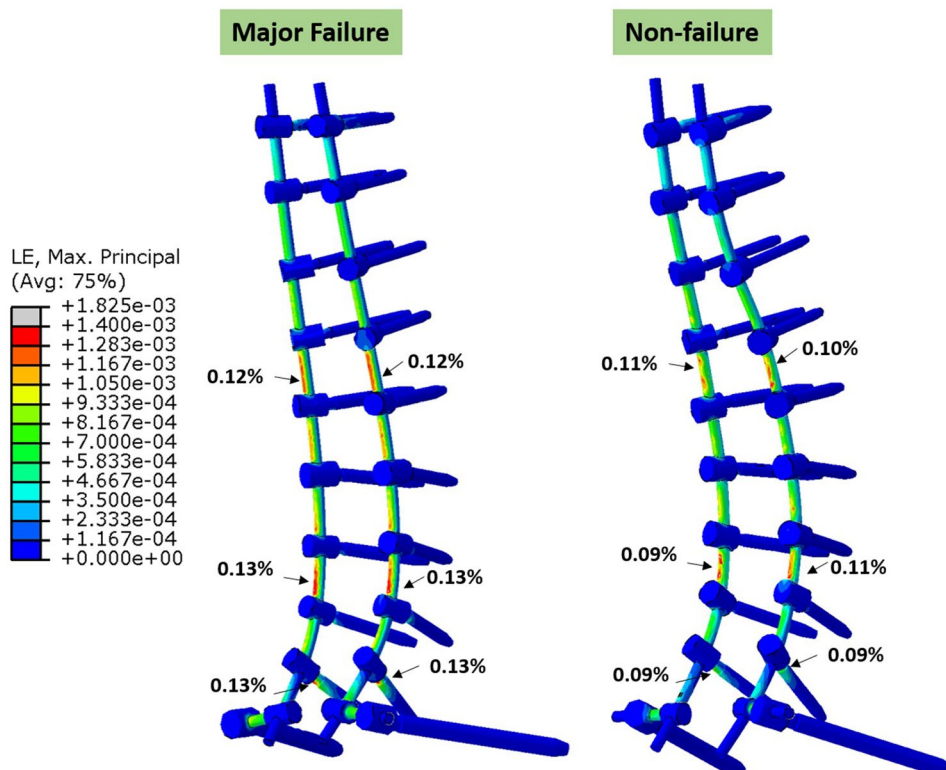
Fig. 5 Rod and screw strain contours under the gravitational loading; values shown are average surface strains (in percentage format)

combination of a PI/LL mismatch (PI minus LL) and SVA can better predict patient disability and provide a guide for appropriate therapeutic decision-making. The difference in PI/LL mismatch between the major failure and non-failure groups was significant (22° vs. 9.3°) (Fig. 1) [3]. As shown in Fig. 3, even when the applied moment is the same, the major failure group observes an increase in rotation and translation. This indicates that the PI/LL mismatch also contributes to the biomechanical stability of the lumbopelvic spine. Surgical intervention to increase LL often involves an osteotomy. One of the most popular osteotomy procedures, PSO, can achieve greater correction at a single segment, with an average correction of 30°–40° [21]. Numerous articles have discussed the benefits and disadvantages of this technique [1, 2, 22]. From a biomechanical point of view, a PSO can improve sagittal balance, thereby decreasing the amount of loading on the spine. However, sharp bending at the apex level—as well as the anatomic nature of the apex relative to gravitational loading—increases the mechanical demand on the implants. Consequently, most RFs are found at the apex in PSO patients [1].

The current study observed high stress/strain concentration at the S1 screws for the major failure cohort. High strain on the S1 screws may result in complications such as screw pullout or pseudarthrosis at the lumbosacral junction for long-segment cases [23]. This result is also consistent with the high rate of S1 screw failure found in the major failure group [3]. In this case, the fixation distal level was

at the pelvic region. The addition of iliac fixation screws serves as temporary scaffolding to allow for the maturation of bony fusion across the lumbosacral junction, which may lower the incidence of screw pull out, L5–S1 pseudarthrosis, and sacral insufficiency fracture at S1–2 [23]. One would expect high load demand on S1 when distal fusion ends at the sacrum [11, 24, 25].

There are some limitations of current model. First, rod contouring was not modeled. Studies have shown that excessive rod bending (e.g., at L5/S1 or at PSO level) are correlated to the high rate of rod fractures [1, 2]. Unfortunately, modeling of rod contouring is extremely difficult in finite element analysis; therefore, it was not included in current study. Second, due to the complexity involved, as well as to a lack of information, muscle forces are neglected in the current model. Very few studies have included muscle force into their models but these studies were still at the earlier stages of incorporing of muscle forces [26, 27]. It was extremely difficult to incorporate muscle force into already complicated models to study the long spinal fusion. However, with the more information and studies of muscle force available to the researchers, we expect that a more robust finite element model can be developed and studied.

This study only looked at the effects of sagittal alignment on the biomechanics of lumbopelvic fixation. This model can be easily modified to look at the effect of posterior bony fixation on the overall mechanical demands on the implants, the effect of anterior column support, rigidity of posterior

or posterolateral fusion mass, the choice of distal fixation level, the effect of rod material or diameter, and the effect of surgical techniques (e.g., PSO, bilateral vs. unilateral). All of these studies would be out of the scope of the focus of the current study, and will be addressed in future analyses.

Conclusion

Due to compensatory differences in the alignment of spinopelvic parameters between normal and failed spines in the presence of a fixed GL, the major failure cohort in this study observed a 20% higher load and 18% greater instability. The higher load and instability increased mechanical demand on the posterior rods in the lower lumbar spine, further emphasizing the importance of proper sagittal alignment, while validating the classification of lumbopelvic fixation failure.

Compliance with ethical standards

IRB statement As this study did not involve human subjects, Institutional Review Board (IRB) approval was not necessary and, therefore, not sought, for the research documented in this manuscript.

References

1. Smith JS, Shaffrey E, Klineberg E et al (2014) Prospective multicenter assessment of risk factors for rod fracture following surgery for adult spinal deformity. J Neurosurg Spine 21:994–1003

2. Barton C, Noshchenko A, Patel V et al (2015) Risk factors for rod fracture after posterior correction of adult spinal deformity with osteotomy: a retrospective case-series. Scoliosis 10:30

3. Cho W, Mason JR, Smith JS et al (2013) Failure of lumbopelvic fixation after long construct fusions in patients with adult spinal deformity: clinical and radiographic risk factors: clinical article. J Neurosurg Spine 19:445–453

4. Berjano P, Bassani R, Casero G et al (2013) Failures and revisions in surgery for sagittal imbalance: analysis of factors influencing failure. Eur Spine J 22(Suppl 6):S853–S858

5. Schwab F, Lafage V, Patel A et al (2009) Sagittal plane considerations and the pelvis in the adult patient. Spine (Phila Pa 1976) 34:1828–1833

6. Kim YC, Lenke LG, Lee SJ et al (2017) The cranial sagittal vertical axis (CrSVA) is a better radiographic measure to predict clinical outcomes in adult spinal deformity surgery than the C7 SVA: a monocentric study. Eur Spine J 26:2167–2175

7. Obeid I, Boniello A, Boissiere L et al (2015) Cervical spine alignment following lumbar pedicle subtraction osteotomy for sagittal imbalance. Eur Spine J 24:1191–1198

8. Glassman SD, Berven S, Bridwell K et al (2005) Correlation of radiographic parameters and clinical symptoms in adult scoliosis. Spine (Phila Pa 1976) 30:682–688

9. Schwab FJ, Smith VA, Biserni M et al (2002) Adult scoliosis: a quantitative radiographic and clinical analysis. Spine (Phila Pa 1976) 27:387–392

10. Protopsaltis TS, Scheer JK, Terran JS et al (2015) How the neck affects the back: changes in regional cervical sagittal alignment correlate to HRQOL improvement in adult thoracolumbar deformity patients at 2-year follow-up. J Neurosurg Spine 23:153–158

11. Emami A, Deviren V, Berven S et al (2002) Outcome and complications of long fusions to the sacrum in adult spine deformity: Luque–Galveston, combined iliac and sacral screws, and sacral fixation. Spine (Phila Pa 1976) 27:776–786

12. Lafage V, Schwab F, Skalli W et al (2008) Standing balance and sagittal plane spinal deformity: analysis of spinopelvic and gravity line parameters. Spine (Phila Pa 1976) 33:1572–1578

13. Le Huec JC, Leijssen P, Duarte M et al (2011) Thoracolumbar imbalance analysis for osteotomy planification using a new method: FBI technique. Eur Spine J 20(Suppl 5):669–680

14. Guan YB, Yoganandan N, Zhang JY, Pintar FA, Cusick JF, Wolfla CE et al (2006) Validation of a clinical finite element model of the human lumbosacral spine. Med Biol Eng Comput 44:633–641

15. Wagner DR, Lotz JC (2004) Theoretical model and experimental results for the nonlinear elastic behavior of human annulus fibrosus. J Orthop Res 22:901–909

16. Wang W, Zhang H, Sadeghipour K et al (2013) Effect of posterolateral disc replacement on kinematics and stress distribution in the lumbar spine: a finite element study. Med Eng Phys 35:357–364

17. Schmidt H, Heuer F, Drumm J et al (2007) Application of a calibration method provides more realistic results for a finite element model of a lumbar spinal segment. Clin Biomech 22(4):377–384

18. Eichenseer PH, Sybert DR, Cotton JR (2011) A finite element analysis of sacroiliac joint ligaments in response to different loading conditions. Spine (Phila Pa 1976) 36:E1446–E1452

19. Lamartina C, Berjano P (2014) Classification of sagittal imbalance based on spinal alignment and compensatory mechanisms. Eur Spine J 23:1177–1189

20. Schwab FJ, Blondel B, Bess S et al (2013) Radiographical spinopelvic parameters and disability in the setting of adult spinal deformity: a prospective multicenter analysis. Spine (Phila Pa 1976) 38:E803–E812

21. Cho KJ, Bridwell KH, Lenke LG et al (2005) Comparison of Smith-Petersen versus pedicle subtraction osteotomy for the correction of fixed sagittal imbalance. Spine (Phila Pa 1976) 30:2030–2037; **discussion 2038**

22. Luca A, Ottardi C, Sasso M et al (2017) Instrumentation failure following pedicle subtraction osteotomy: the role of rod material, diameter, and multi-rod constructs. Eur Spine J 26:764–770

23. Saigal R, Lau D, Wadhwa R et al (2014) Unilateral versus bilateral iliac screws for spinopelvic fixation: are two screws better than one? Neurosurg Focus 36:E10

24. Youssef JA, Orndorff DO, Patty CA et al (2013) Current status of adult spinal deformity. Global Spine J 3:51–62

25. Yasuda T, Hasegawa T, Yamato Y et al (2016) Lumbosacral junctional failures after long spinal fusion for adult spinal deformity—Which vertebra is the preferred distal instrumented vertebra? Spine Deform 4:378–384

26. Rohlmann A, Bauer L, Zander T, Bergmann G, Wilke HJ (2006) Determination of trunk muscle forces for flexion and extension by using a validated finite element model of the lumbar spine and measured in vivo data. J Biomech 39(6):981–989

27. Zander T, Rohlmann A, Calisse J, Bergmann G (2001) Estimation of muscle forces in the lumbar spine during upper-body inclination. Clin Biomech 16:S73–S80